

Cooperativity in sandpiles: statistics of bridge geometries

Anita Mehta[†], G C Barker[‡], and J M Luck[§]

[†] S N Bose National Centre for Basic Sciences, Block JD, Sector 3, Salt Lake,
Calcutta 700098, India

[‡] Institute of Food Research, Colney Lane, Norwich NR4 7UA, UK

[§] Service de Physique Théorique[‡], CEA Saclay, 91191 Gif-sur-Yvette cedex, France

Abstract. Bridges form dynamically in granular media as a result of spatiotemporal inhomogeneities. We classify bridges as linear and complex, and analyse their geometrical characteristics. In particular, we find that the length distribution of linear bridges is exponential. We then turn to the analysis of the orientational distribution of linear bridges and find that, in three dimensions, they are *vertically diffusive but horizontally superdiffusive*; thus, when they exist, long linear bridges form ‘domes’. Our results are in good accord with Monte Carlo simulations of bridge structure; we make predictions for quantities that are experimentally accessible, and suggest that bridges are very closely related to force chains.

PACS numbers: 45.70.-n, 61.43.Gt, 89.75.Fb, 05.65.+b, 05.40.-a

E-mail: anita@bose.res.in, barker@bbsrc.ac.uk, luck@spht.saclay.cea.fr

1. Introduction

The surface of a sandpile cloaks within it a vast array of complex structures – networks of grains whose stability is interconnected, surrounded by pores and necks of void space. Bridges – arch-like structures, where mutual stabilisation is a principal ingredient – are prime among these, spanning all manner of shapes and sizes through a granular medium. They can be stable for arbitrarily long times, since the Brownian motion that would dissolve them away in a liquid is absent in sandpiles – grains are simply too large for the ambient temperature to have any effect. As a result, they can affect the ensuing dynamics of the sandpile; a major mechanism of compaction is the gradual collapse of long-lived bridges in weakly vibrated granular media, resulting in the disappearance of the voids that were earlier enclosed [1]. Bridges are also responsible for the ‘jamming’ [2] that occurs, for example, as grains flow out of a hopper.

The difficulty of even identifying, leave alone analysing, structures as complex as bridges in a three-dimensional assembly should not be underestimated; such an algorithm now exists, and its use has resulted in the identification and classification of a panoply of bridge configurations generated via numerical simulations [3, 4]. However, even given the presence of such data, it is a far from obvious task to cast it in theoretical terms. In the following, we present a theory for the formation of bridges, which, among other things, is able to explain at least some of the salient features of our numerical data.

We first define a bridge. Consider a stable packing of hard spheres under gravity, in three dimensions. Each particle typically rests on three others which stabilise it. *A bridge is a configuration of particles in which the three-point stability conditions of two or more particles are linked; that is, two or more particles are mutually stabilised.* They are thus structures which cannot be formed by the *sequential* placement of individual particles; they are, however, frequently formed by natural processes such as shaking and pouring, where cooperative effects arise naturally. In a typical packing, upto 70 percent of particles are involved in bridge configurations. The detailed history of a stabilisation process identifies a unique set of bridges, since the stabilising triplet for each sphere is well defined. While it is impossible to determine bridge distributions uniquely from an array of coordinates representing particle positions, we are able via our algorithm to obtain ones that are the most likely to be the result of a given stabilisation process [3, 4].

We now distinguish between *linear* and *complex* bridges via a comparison of Figures 1 and 2. Figure 1 illustrates a *complex* bridge, i.e., a mutually stabilised cluster of five particles, where the stability is provided by six stable base particles. (Of course the whole is embedded in a stable network of grains within the sandpile.) Also shown is the network of contacts for the particles in the bridge: we see clearly that three of the particles each have two mutual stabilisations. Figure 2 illustrates a seven particle linear bridge with nine base particles. The contact network shows that this bridge has a simpler topology than that in Figure 1; here, all of the mutually stabilised particles are in sequence, as in a string. This is an example of a *linear* bridge.

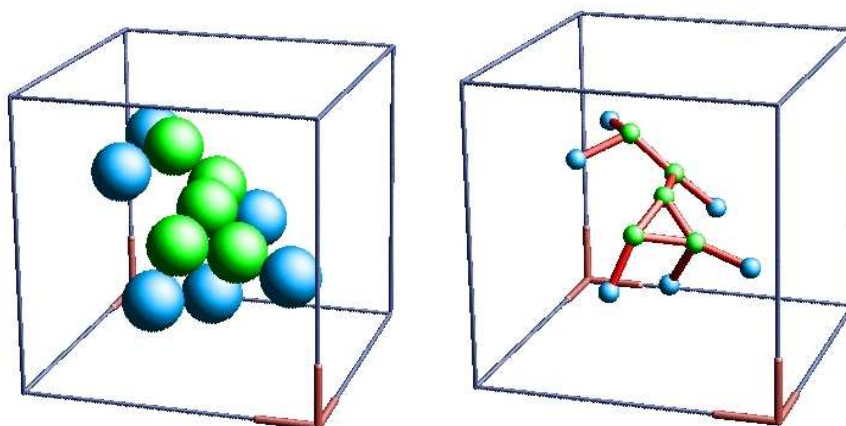


Figure 1. A five particle *complex bridge*, with six base particles (left), and the corresponding contact network (right).

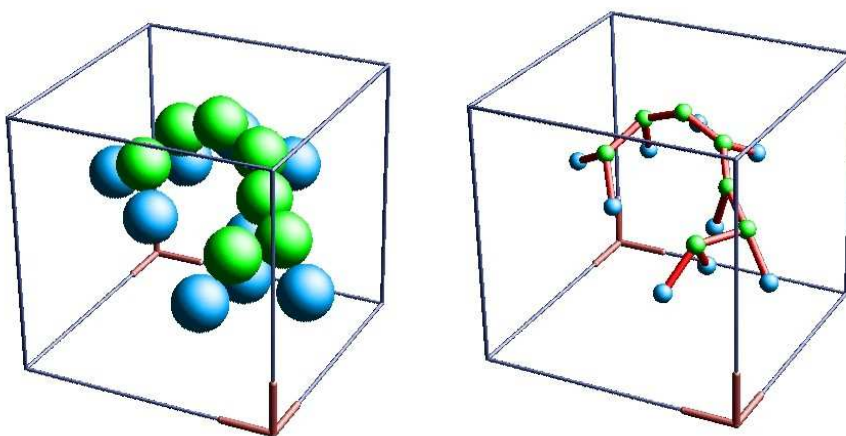


Figure 2. A seven particle *linear bridge* with nine base particles (left), and the corresponding contact network (right).

An important point to note is that bridges can only be formed sustainably in the presence of friction; the mutual stabilisations needed would be unstable otherwise! Although we use Monte Carlo simulations (described below) which do not contain friction explicitly, the configurations we generate correspond to those in nature that include frictional effects. In particular, they generate coordination numbers in a range that is consistent with the presence of friction [1, 5, 6]. Additionally, we have analysed the configurations of molecular dynamics simulations in the limit of high friction[§]; these generate distributions of bridges very similar to our own. Our simulations suggest

[§] We thank Leo Silbert for letting us use configurations generated from his molecular dynamics simulations, where we have found and analysed the distribution of bridges.

strong analogies between bridge structure and force distributions [7] in granular media, indicating that bridges might be complementary (and experimentally easier) probes of inhomogeneities in these systems.

2. Simulation details

We have simulated the shaking of hard spheres by using an algorithm whose main modelling ingredients involve *stochastic* grain displacements and *collective* relaxation from them [1]. This has three distinct stages.

- (1) The assembly is dilated in a vertical direction (with free volume being introduced homogeneously throughout the system), and each particle is given a random horizontal displacement; this models the dilation phase of a vibrated granular medium.
- (2) The packing is compressed in a uniaxial external field representing gravity, using a low-temperature Monte Carlo process.
- (3) The spheres are stabilised using a steepest descent ‘drop and roll’ dynamics to find a local minimum of the potential energy.

Steps (2) and (3) model the quench phase of the vibration, where particles relax to locally stable positions in the presence of gravity. Crucially, during the third phase, the spheres are able to roll in contact with others; *mutual stabilisations* are thus allowed to arise, mimicking collective effects. The final configuration has a well-defined network of contacts, with each sphere satisfying a uniquely defined three-point stability criterion.

Restructuring simulations are performed in a rectangular cell with lateral periodic boundaries, and a hard disordered base. The simulations, performed serially on a desktop workstation, have a very time-consuming Monte Carlo compression phase with each simulation taking several days’ worth of CPU time. This is necessary in order to have simulation results which are reproducible, without appreciable dependence on Monte Carlo parameters or system size.

Our previous investigations [1, 3, 4] have a steady state described by particular values for structural descriptors such as the mean packing fraction and the mean coordination number. Typically the steady-state mean volume fraction is in the range $\Phi \sim 0.55 - 0.61$. The mean coordination number is always $Z \approx 4.6 \pm 0.1$. Since for frictional packings the minimal coordination number is $Z = d + 1$ [5], this confirms that our 3D configurations correspond to those generated in the presence of friction. In fact, the mean coordination number of molecular dynamics configurations of frictional sphere packings is slightly above 4.5, in the limit of a large friction coefficient [6].

Each of our configurations includes about $N_{\text{tot}} = 2200$ particles. We have examined approximately 100 configurations from the steady states of the reorganisation process for the following two values of the packing fraction: $\Phi = 0.56$ and $\Phi = 0.58$. Segregation is avoided by choosing monodisperse particles: a rough base prevents ordering. A large number of restructuring cycles is needed to reach the steady state for a given

shaking amplitude: about 100 stable configurations (picked every 100 cycles in order to avoid correlation effects) are saved for future analysis. From these configurations, and following specific prescriptions, our algorithm identifies bridges as clusters of mutually stabilised particles [3, 4].

Figure 3 illustrates two characteristic descriptors of bridges used in this work. Along the lines of [4], the *main axis* of a bridge is defined using triangulation of its base particles. Triangles are constructed by choosing all possible connected triplets of base particles: the vector sum of their normals is defined to be the direction of the main axis of the bridge. The orientation angle Θ is defined as the angle between the main axis and the z -axis. The *base extension* b is defined as the radius of gyration of the base particles about the z -axis (which is thus distinct from the radius of gyration about the main axis of the bridge).

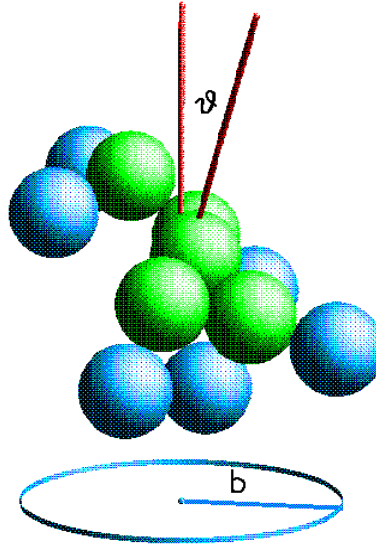


Figure 3. Definition of the angle Θ and the base extension b of a bridge. The main axis makes an angle Θ with the z -axis; the base extension b is the projection of the radius of gyration of the bridge on the x - y plane.

3. Geometrical characteristics. Size and diameter distribution

Bridge formation in the presence of a shaking intensity is of course a dynamical process; we, however, adopt an ergodic viewpoint [8] here, looking at ensemble statistics of bridges generated by our simulations, at a given density of packing. Although we present statistics for both linear and complex bridges, we analyse the former in greater detail,

both because they are conceptually simpler and because they are in fact more numerous in our simulations [3, 4].

We first address the question of the length distribution of linear bridges. Our simulations show that as a linear bridge gets longer, it is increasingly likely to get branched, i.e., to become complex [3, 4]. Defining the length distribution f_n as the probability that a linear bridge consists of exactly n spheres, we expect therefore that a bridge of size n remains linear with a probability $p < 1$ if an $(n + 1)^{\text{th}}$ sphere is added to it, hence

$$f_n = (1 - p)p^n. \quad (3.1)$$

Equation (3.1) says that the length distribution of linear bridges is exponential; interestingly, this law governs also the size distribution of 1D percolation clusters [9], suggesting that linear bridges (despite being embedded in 3D) can really be regarded as random ‘strings’ of length n .

We can also derive the exponential law by using a continuum approach; we do this below, largely to introduce a formalism that will be extensively used later. A linear bridge is modelled as a continuous curve or ‘string’, parametrised by the arc length s from one of its endpoints. The length distribution $f(s)$ is the probability density that the total length of the curve is s ; we assume that a linear bridge disappears at a constant rate α per unit length, either by changing from linear to complex or by collapsing. The probability $S(s)$ that a given bridge survives at least up to length s thus obeys the rate equation

$$\dot{S}(s) = -\alpha S(s), \quad (3.2)$$

where the dot stands for a derivative with respect to s . This gives an exponential decay $S(s) = \exp(-\alpha s)$ of the survival probability, so that the probability distribution of the length s of linear bridges, $f(s) = -\dot{S}(s)$, reads

$$f(s) = \alpha \exp(-\alpha s), \quad (3.3)$$

in agreement with the earlier prediction (3.1).

Figure 4 shows a logarithmic plot of numerical data for the length distribution f_n of linear bridges. The data exhibit an exponential fall off of the form (3.1), with $p \approx 0.37$, i.e., $\alpha \approx 0.99$ ||. This exponential decay of the distribution of linear bridges is clearly seen until $n \approx 12$.

Complex bridges begin to be dominant around $n \approx 8$. For a complex bridge, the number n is now referred to as the ‘size’ of the bridge. As complex bridges are branched objects, we now expect a power-law fall-off of the size distribution:

$$f_n \sim n^{-\tau}, \quad (3.4)$$

in analogy with the statistics of random branched objects, such as critical percolation clusters in higher dimensions [9]. The power law (3.4) is observed on the numerical data

|| Despite its proximity to unity, this value of α has no special significance, as can be seen from the corresponding value of p .

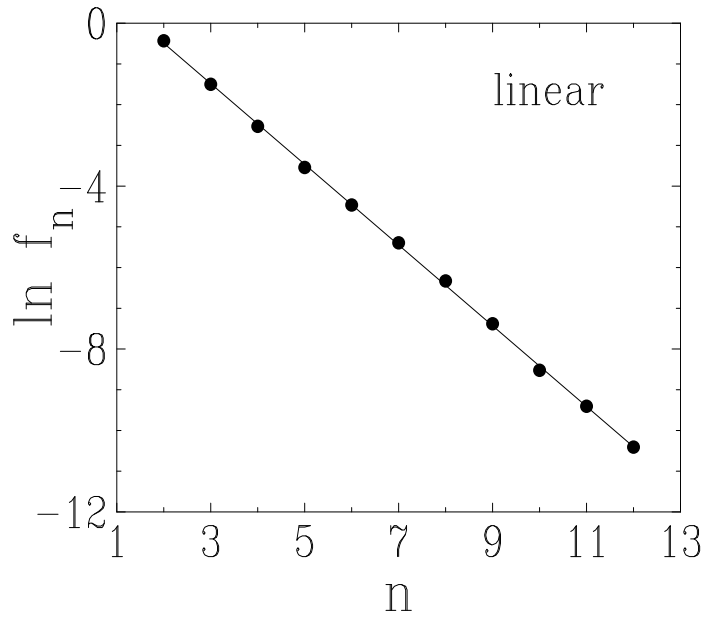


Figure 4. Logarithmic plot of the length distribution f_n of linear bridges, against n , for $\Phi = 0.58$. Full line: least-square fit yielding $p \approx 0.37$, i.e., $\alpha \approx 0.99$.

shown in Figure 5. The measured value of the exponent τ seems to coincide with the limiting value $\tau = 2$, below which the mean size $\langle n \rangle = \sum n f_n$ is divergent.

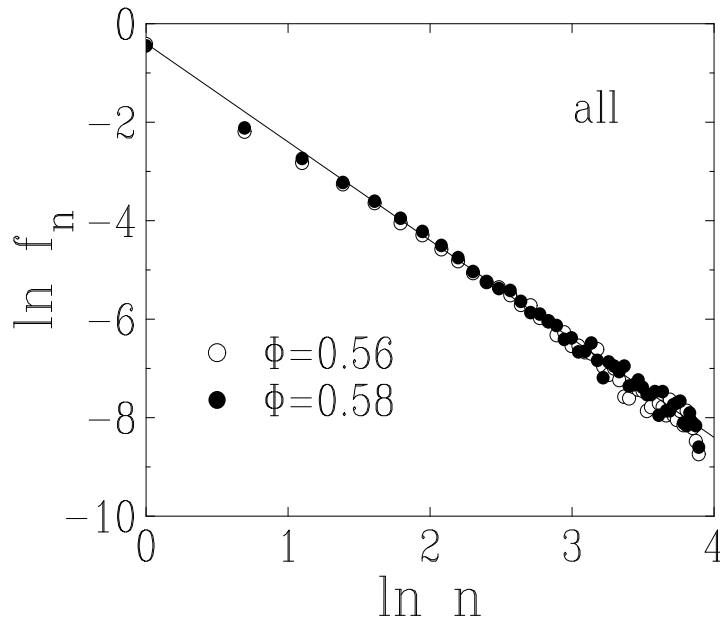


Figure 5. Log-log plot of the size distribution f_n of all bridges, against n , for two volume fractions. This distribution is dominated by complex bridges, since these predominate after $n \sim 8$. Full line: least-square fit yielding $\tau \approx 2.00$.

We now turn to the diameter of linear and complex bridges, which is one of the most important of their geometrical characteristics. The typical diameter R_n of a bridge of size n is such that R_n^2 is the mean squared end-to-end distance over all the bridges of size n . We examine this quantity separately for linear bridges, as well as the ensemble of all bridges. In both cases we expect and find a power-law behaviour

$$R_n \sim n^\nu. \quad (3.5)$$

For linear bridges, $D_{\text{lin}} = 1/\nu_{\text{lin}}$ can be interpreted as their fractal dimension. The observed value (see Figure 6) $\nu_{\text{lin}} \approx 0.66$, i.e., $D_{\text{lin}} \approx 1.51$, lies between those for a self-avoiding walk in two ($\nu_2 = 3/4$) and three ($\nu_3 \approx 0.59$) dimensions. This seems entirely reasonable, since linear bridges in three dimensions are likely to have an effective dimensionality between 2 and 3: they may start off confined to a plane, and then collapse onto each other, due to the effects of vibration.

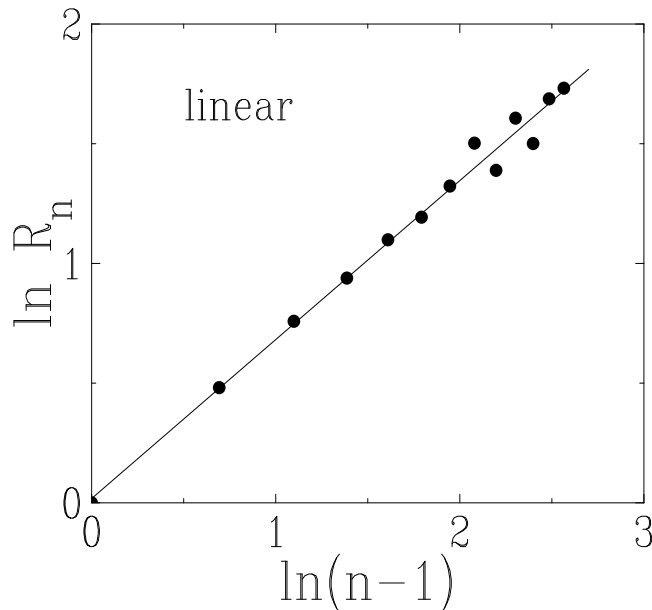


Figure 6. Log-log plot of the typical diameter R_n of linear bridges, against $n-1$, the number of mutually stabilising bonds, for $\Phi = 0.58$. Full line: least-square fit yielding $\nu_{\text{lin}} \approx 0.66$, i.e., $D_{\text{lin}} \approx 1.51$.

For complex bridges, we again find a power law of the form (3.5), where the geometrical exponent $\nu_{\text{all}} \approx 0.74$ (see Figure 7) can be compared with the corresponding value $\nu \approx 0.875$ for 3D percolation [9]. (Although the figure shows statistics for ‘all’ bridges, these mostly reflect the behaviour of complex bridges, which dominate beyond about $n \approx 8$.)

Lastly, we plot in Figure 8 the probability distribution function of the base extension b , for linear bridges; this is clearly a measure of the spanning, and hence the jamming, potential of a bridge (see Figure 3). We plot also in Figure 8 distribution functions that are conditional on the bridge size n . This was done to compare our

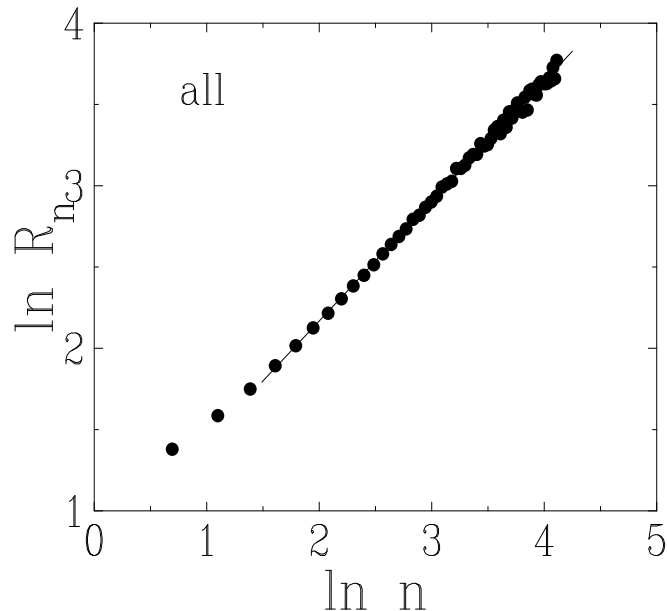


Figure 7. Log-log plot of the typical diameter R_n of all bridges, against size n , for $\Phi = 0.58$. These statistics mainly derive from complex bridges, which dominate beyond about $n \approx 8$. Full line: least-square fit to points with $n > 5$, yielding $\nu_{\text{all}} \approx 0.74$.

results with those of [10], bearing in mind of course that our results refer to sphere packings in three dimensions whereas theirs refer to disk packings in two. In our case, the conditional distributions are sharply peaked, and only extend over a finite range of b ; in theirs the peaks are smaller and the distributions broader. Our results indicate that at least in three dimensions, and upto the lengths of linear bridges probed, bridges of a given length n have a fairly characteristic horizontal extension; we can predict fairly reliably the dimension of the orifice that they might be expected to jam. The results of [10] indicate, on the contrary, that there is a wide range of orifices which would be jammed by disk packings of a given length, in two dimensions. Also, for our three-dimensional bridges, the cumulative distribution has a long tail at large extensions, reflecting chiefly the existence of larger bridges than in the data of [10]. All of this seems entirely reasonable given the more complex topology of three-dimensional space, as well as the greater diversity of possible sphere packings within it.

In the lower part of Figure 8 we have plotted the logarithm of the probability distribution of base extensions against the normalised variable $b/\langle b \rangle$, where $\langle b \rangle$ is the mean extension of bridge bases. This figure emphasises the exponential tail of the distribution function, and also shows that bridges with small base extensions are unfavoured. It is interesting to note that the form of the normalised distribution resembles that found in force distributions of emulsions [11], and that there are also similarities with normal force distributions in MD simulations of particle packings (see e.g. [7, 12]). In our simulations, the sharp drop at the origin with a very

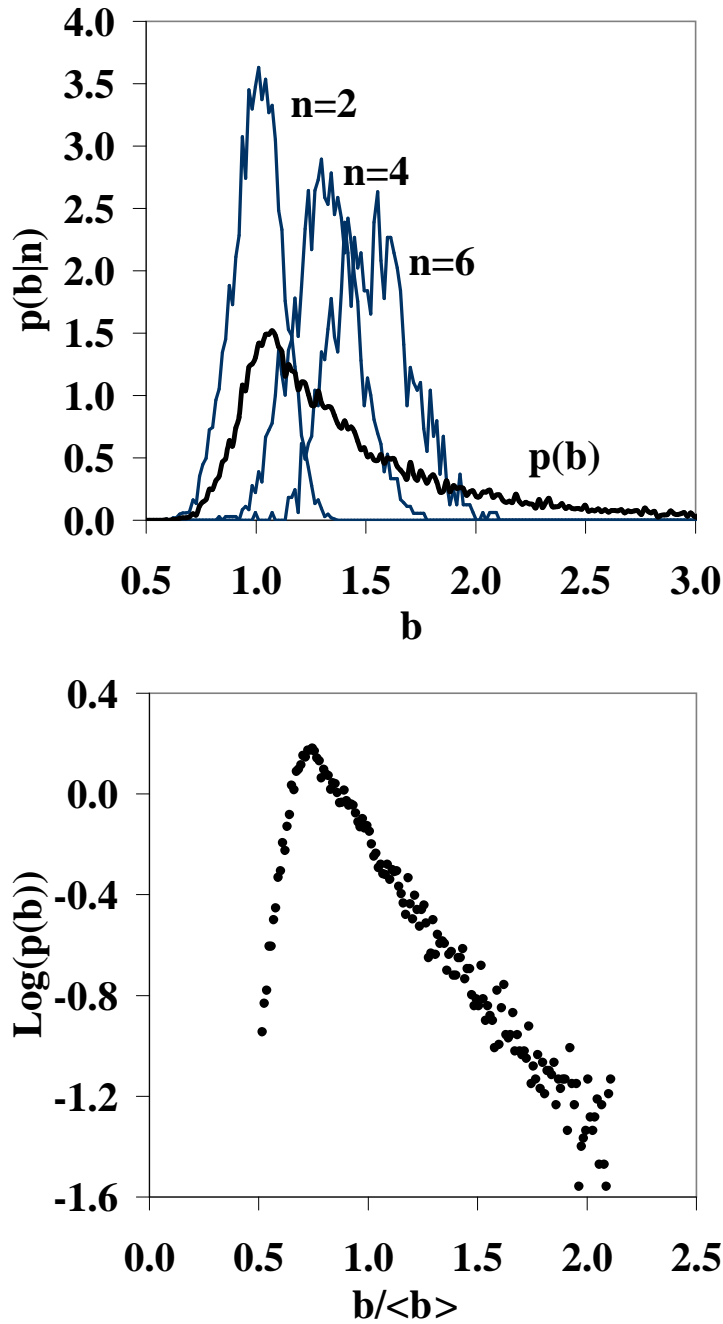


Figure 8. Distribution of base extensions of bridges, for $\Phi = 0.58$. The top panel also shows the distributions conditional on the bridge size n , for $n = 2, 4, 6$. The bottom panel shows the logarithm of the distribution as a function of the normalised variable $b/\langle b \rangle$.

tangible peak strongly resembles that obtained in the latter case, in the limit of strong deformations [7]. Realising that the measured forces [7, 11] propagate through chains of particles, we use this similarity to suggest that our bridges are really just long-lived force chains, which have survived despite strong deformations. We suggest also that

with the current availability of 3D visualisation techniques such as NMR [13], bridge configurations might be an easily measurable, and effective, tool to probe inhomogeneous force networks in shaken sand.

4. Orientational distribution of linear bridges. Theory and simulation

Linear bridges predominate at small n , which is after all the regime of interest for finite-sized simulations and experiments. The theory we present below focuses on such bridges; the distribution of their orientation is predicted, and then compared with our simulation results.

As before, a linear bridge is modelled as a continuous curve, parametrised by the arc length s from one of its endpoints. We consider both the local or ‘link’ angle $\theta(s)$ between the direction of the tangent to the bridge at point s and the horizontal, and the mean angle made by the bridge from its origin up to point s ,

$$\Theta(s) = \frac{1}{s} \int_0^s \theta(u) du. \quad (4.1)$$

As the length of the bridge increases, our simulations [3, 4] show that, while the local angle $\theta(s)$ may vary in a random fashion, the angle $\Theta(s)$ usually decreases with s . Small linear bridges are almost never flat [3, 4]; as they get longer, assuming that they still stay linear, they get ‘weighed down’, arching over as at the mouth of a hopper [14]. Thus, in addition to our earlier claim that long linear bridges are rare, we claim further here that (if and) when they exist, they typically have flat bases, becoming ‘domes’.

We use these insights to write down equations to investigate the angular distribution of linear bridges. These couple the evolution of the local angle $\theta(s)$ with local density fluctuations $\phi(s)$ at point s :

$$\dot{\theta} = -a\theta - b\phi^2 + \Delta_1\eta_1(s), \quad (4.2)$$

$$\dot{\phi} = -c\phi + \Delta_2\eta_2(s). \quad (4.3)$$

The effects of vibration on each of θ and ϕ are represented by two independent white noises $\eta_1(s)$, $\eta_2(s)$, such that

$$\langle \eta_i(s)\eta_j(s') \rangle = 2\delta_{ij}\delta(s-s'), \quad (4.4)$$

whereas the parameters a, \dots, Δ_2 are assumed to be constant.

The phenomenology behind the above equations is the following: the evolution of $\theta(s)$ is caused by the addition to the bridge of single particles moving independently. The motion of particles within their cages gives rise to the fluctuations of local density at a point s ; thus ϕ can be regarded as an effective *collective* coordinate, with θ seen as an *independent-particle* coordinate.¶. The individual dynamics are simple: the first terms on the right-hand side of (4.2), (4.3) say that neither θ nor ϕ is allowed to be arbitrarily large. Their coupling via the second term in (4.2) arises as follows: large link

¶ The evolution of ϕ is thus implicitly slower than that of θ – we do not use this fact here, but will do so in future work where these degrees of freedom will be strongly coupled.

angles θ will be increasingly unstable in the presence of density fluctuations ϕ^2 of large magnitude, which would to a first approximation ‘weigh the bridge down’, i.e., decrease the angle θ locally. Similar coupled equations have been written down for other aspects of sandpile dynamics, to do with the coupling of independent-particle and collective coordinates [15].

Reasoning as above, we therefore anticipate that for low-intensity vibrations and stable bridges, both density fluctuations $\phi(s)$ and link angles $\theta(s)$ will be small. Accordingly, we linearise (4.2), obtaining thus an Ornstein-Uhlenbeck equation [16, 17]

$$\dot{\theta} = -a\theta + \Delta_1 \eta_1(s). \quad (4.5)$$

Numerical results (see below) suggest that the initial angle θ_0 , i.e., that observed for very small bridges, is itself Gaussian with variance $\sigma_0^2 = \langle \theta_0^2 \rangle$. The angle $\theta(s)$ is then a Gaussian process with zero mean and correlation

$$\langle \theta(s)\theta(s') \rangle = \sigma_{\text{eq}}^2 e^{-a|s-s'|} + (\sigma_0^2 - \sigma_{\text{eq}}^2) e^{-a(s+s')}. \quad (4.6)$$

The characteristic length for the decay of orientation correlations is $\xi = 1/a$, and the variance of the link angle reads

$$\langle \theta^2 \rangle(s) = \sigma_{\text{eq}}^2 + (\sigma_0^2 - \sigma_{\text{eq}}^2) e^{-2as}, \quad (4.7)$$

where

$$\sigma_{\text{eq}}^2 = \frac{\Delta_1^2}{a} \quad (4.8)$$

is the ‘equilibrium’ value of the variance of the link angle. Thus as the chain gets longer, the variance of the link angle relaxes from σ_0^2 (that for the initial link) to σ_{eq}^2 , in the limit of an infinite bridge.

We predict from the above that the mean angle $\Theta(s)$ will have a Gaussian distribution, for any fixed length s . By inserting (4.6) into (4.1), we derive its variance:

$$\langle \Theta^2 \rangle(s) = 2\sigma_{\text{eq}}^2 \frac{as - 1 + e^{-as}}{a^2 s^2} + (\sigma_0^2 - \sigma_{\text{eq}}^2) \frac{(1 - e^{-as})^2}{a^2 s^2}. \quad (4.9)$$

The asymptotic result

$$\langle \Theta^2 \rangle(s) \approx \frac{2\sigma_{\text{eq}}^2}{as} \approx \frac{2\Delta_1^2}{a^2 s} \quad (4.10)$$

confirms our earlier statement (see below (4.1)) that a typical long bridge has a base that is almost flat. It can be viewed as consisting of a large number $as = s/\xi \gg 1$ of independent ‘blobs’⁺, each of length ξ .

The result (4.10) has another interpretation. As $\theta(s)$ is small with high probability for a very long bridge, its extension in the vertical direction reads approximately

$$Z = z(s) - z(0) \approx s \Theta(s), \quad (4.11)$$

⁺ This is qualitatively reminiscent of a similar problem in polymers, where the de Gennes picture of ‘blob’ dynamics in dilute solutions gives way to rigid rod-like behaviour – see e.g. [18].

so that $\langle Z^2 \rangle \approx s^2 \langle \Theta^2 \rangle (s) \approx 2(\Delta_1/a)^2 s$. Going back to the discrete formalism, we have therefore

$$Z_n \sim n^{1/2}. \quad (4.12)$$

The vertical extension of a linear bridge is thus found to grow with the usual random-walk exponent $1/2$, whereas its horizontal extension exhibits the non-trivial exponent $\nu_{\text{lin}} \approx 0.66$ of Figure 6. Thus, *long linear bridges are domelike; they are vertically diffusive but horizontally superdiffusive*. We recall that the two-dimensional arches found in [10] were diffusive in a vertical direction; our present results show that in three dimensions, the vertical diffusivities of bridge structures remain, and are enriched by a horizontal superdiffusivity. Evidently, jamming in a three-dimensional hopper would be caused by the planar projection of such a *dome*.

We now compare these predictions with data from our simulations. The numerical data shown in Figure 9 confirm that the mean angle has, to a good approximation, a Gaussian distribution. It has been checked to high accuracy (less than 2 percent for a bin size $\delta\varphi = 5$ degrees) that the azimuthal angle φ of the main bridge axis has the expected flat distribution. Figure 10 shows the size dependence of the variance $\langle \Theta^2 \rangle (s)$. The numerical data for two values of the packing fraction are found to agree rather well with the first (stationary) term of (4.9), with a common value of the parameters $\sigma_{\text{eq}}^2 = 0.093$ and $a = 0.55$.

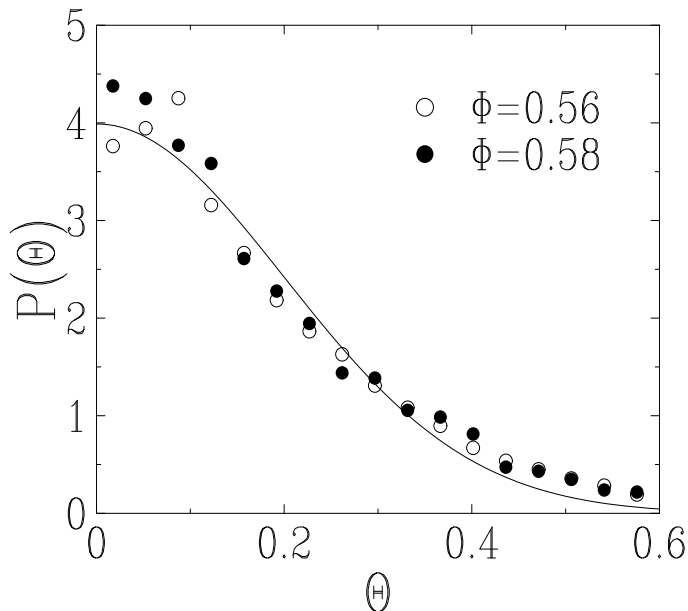


Figure 9. Plot of the normalised distribution of the mean angle Θ (in radians) of linear bridges of size $n = 4$, for both volume fractions. The $\sin \Theta$ Jacobian has been duly divided out, explaining thus the larger statistical errors at small angles. Full lines: common fit to (half) a Gaussian law.

We conclude this section with the following remarks. First, more subtle effects, including the effects of transients via the second term of (4.9), and the dependence

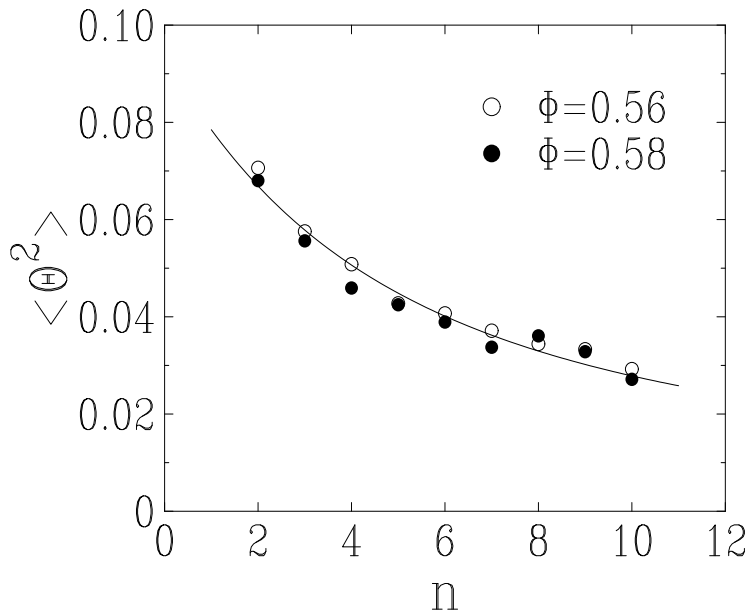


Figure 10. Plot of the variance of the mean angle of a linear bridge, against size n , for both volume fractions. Full line: common fit to the first (stationary) term of (4.9), yielding $\sigma_{\text{eq}}^2 = 0.093$ and $a = 0.55$.

of the parameters σ_{eq}^2 and a on the packing fraction Φ , are deserving of further investigation. Secondly, with increasing Φ , it is more and more rare for bridge formation to proceed ‘sequentially’, i.e., with the progressive attachment of independent blobs to the bridge. The current picture should therefore cease to hold at a limit packing fraction Φ_{lim} , which is reminiscent of the *single-particle relaxation threshold density* [19], at which the dynamics of granular compaction crosses over from being single-particle (sequential) to collective. Finally, while we have allowed for the local variability of density fluctuations ϕ via (4.3), we have so far not explicitly coupled these to bridge orientations in our solutions. All of these issues form part of ongoing work, since much more numerical data is needed before a comparison with our theory is possible.

5. Discussion

In the above, we have classified bridge structures in granular media as either linear or complex, analysed their structures as obtained in our simulations, and obtained values for some of their more important geometrical exponents. We have also presented a theory for their orientational correlations, which is in reasonably good agreement with our simulations, and more importantly, makes predictions that can be observed experimentally. Do linear bridges really predominate at short lengths? Do they really cross over to being domelike at large lengths, if they survive? The answers to these and other questions, if obtained experimentally, will not just satisfy what is arguably mere scientific curiosity. Our investigations above suggest that *long-lived bridges are natural*

indicators of sustained inhomogeneities in granular systems. Consequently, experimental and theoretical explorations of geometry and dynamics in stable bridge networks will have immediate implications for issues such as hysteresis and cooperative stability, which are some of the most visible manifestations of complexity in granular media.

Acknowledgments

AM warmly thanks SMC-INFM (Research and Development Center for Statistical Mechanics and Complexity, Rome, Italy), and the Service de Physique Théorique, CEA Saclay, where parts of this work were done. GCB acknowledges support from the Biotechnology and Biological Sciences Research Council UK and thanks Luis Pugnali for help with the figures. Kirone Mallick is gratefully acknowledged for fruitful discussions.

References

- [1] Mehta A and Barker G C 1991 Phys. Rev. Lett. **67** 394
Barker G C and Mehta A 1992 Phys. Rev. A **45** 3435
- [2] Jaeger H M, Nagel S R, and Behringer R P 1996 Rev. Mod. Phys. **68** 1259
de Gennes P G 1999 Rev. Mod. Phys. **71** S374
- [3] Pugnali L A, Barker G C, and Mehta A 2001 Adv. Complex Syst. **4** 289
- [4] Pugnali L A and Barker G C 2004 Physica A **337** 428
- [5] Edwards S F 1998 Physica **249** 226
- [6] Silbert L E *et al* 2002 Phys. Rev. E **65** 031304
- [7] Erikson J M *et al* 2002 Phys. Rev. E **66** 040301
O'Hern C S *et al* 2002 Phys. Rev. Lett. **88** 075507
- [8] Edwards S F 2003 in *Challenges in Granular Physics* edited by Mehta A and Halsey T C (Singapore: World Scientific)
- [9] Stauffer D and Aharony A 1992 *Introduction to Percolation Theory* 2nd ed (London: Taylor and Francis)
- [10] To K, Lai P Y, and Pak H K 2001 Phys. Rev. Lett. **86** 71
- [11] Brujic J *et al* 2003 Physica A **327** 201
- [12] O'Hern C S *et al* 2001 Phys. Rev. Lett. **86** 111
Landry J W *et al* 2003 Phys. Rev. E **67** 041303
- [13] see chapters by Fukushima E and Seidler G T *et al* 2003 in *Challenges in Granular Physics* edited by Mehta A and Halsey T C (Singapore: World Scientific)
- [14] Brown R L and Richards J C 1966 *Principles of Powder Mechanics* (Oxford: Pergamon)
- [15] Mehta A, Luck J M, and Needs R J 1996 Phys. Rev. E **53** 92
Hoyle R B and Mehta A 1999 Phys. Rev. Lett. **83** 5170
- [16] Uhlenbeck G E and Ornstein L S 1930 Phys. Rev. **36** 823
Wang M C and Uhlenbeck G E 1945 Rev. Mod. Phys. **17** 323
- [17] van Kampen N G 1992 *Stochastic Processes in Physics and Chemistry* (Amsterdam: North-Holland)
- [18] Doi M and Edwards S F 1986 *The Theory of Polymer Dynamics* (Oxford: Clarendon)
- [19] Berg J and Mehta A 2001 Europhys. Lett. **56** 784